ISBN: 978-3-95450-234-9 ISSN: 2673-5504 doi:10.18429/JACoW-SRF2023-MOPMB021

CORRELATING LAMBDA SHIFT MEASUREMENTS WITH RF PERFORMANCE IN MID-T HEAT TREATED CAVITIES

R. Ghanbari*, M. Wenskat, R. Monroy-Villa, G. Kacha Deyu, W. Hillert
Institute of Experimental Physics, University of Hamburg, Hamburg, Germany
J. Wolff, C. Bate, L. Steder, D. Reschke, Deutsches Elektronen-Synchrotron DESY, Germany

Abstract

Heat treatment procedures have been identified as crucial for the performance of niobium SRF cavities, which are the key technology of modern accelerators. The so called "mid-T heat treatments", invert the dependence of losses on the applied accelerating field (anti-Q slope) and significantly reduce the absolute value of losses. The mechanism behind these improvements is still under investigation, and further research is needed to fully understand the principle processes involved. Anomalies in the frequency shift near the transition temperature (T_c), known as "dip" can provide insight into fundamental material properties and allow us to study the relationship of frequency response with surface treatments. Therefore, we have measured the frequency versus temperature of multiple mid-T heat treated cavities with different recipes and studied the correlation of SRF properties with frequency shift features. The maximum quality factor correlates with two such shift features, namely the dip magnitude per temperature width and the total frequency shift.

INTRODUCTION

Superconducting radio-frequency (SRF) cavity research opens doors to fascinating discoveries and technological advancements in modern accelerators field. Understanding the role of impurities in the RF layer, which is approximately the first 200 nm of the cavity surface, is crucial for optimizing the RF performance [1,2]. Mid-T heat treatment, a surface treatment which is defined as heating for 3-20 hours (h) at 200-400 °C in Ultra High Vacuum (UHV), utilizes the diffusion of oxygen from the native niobium oxide and increases the concentration of oxygen impurities into the RF layer [3–6]. It enhances high quality factor (Q_0) values of up to 4.2×10^{10} at 20 MV/m with showing anti-Q slope, along with an average maximum accelerating field around 24-30 MV/m, where few cavities achieved more than 30 MV/m [7–10]. Previous reports have explored main characteristic of mid-T heat treated cavities, particularly focusing on the Q_0 in relation to the E_{acc} to study the principals responsible for their exceptional performance [1, 2, 11–14]. While much attention has been given to Q_0 and surface resistance (R_s), fewer studies have explored the behavior of frequency shift of cavities as a function of temperature (df vs. T), which holds valuable insights into the surface reactance (X_s) and the behavior of superconducting carriers. Recent theoretical studies have started to model the frequency response of SRF cavities, and have sparked ongoing studies to identify the underlying processes [15]. Remarkably, dip features show variations based on the surface treatment, and correlations with cavity performance are found [1, 2]. Despite the recent progress achieved, several questions remain, such as how the impurity concentrations [16–19], especially the oxygen profile, relate to the observed changes in RF performance. The potential application of these findings extends across multiple applications, from accelerator technology to dark matter detection and quantum information technology, propelling scientific and technological progress in diverse fields with reducing BCS resistance (R_{BCS}) and residual resistance (R_{res}) [1–10]. Here, we aim to investigate the features of dip phenomenon resulting from the mid-T heat treatment on the surface of SRF cavities and correlate them with RF performance and oxygen diffusion.

EXPERIMENTAL

The most commonly employed method, also used in this study, is the S21 measurement, which measures the transmitted signal at the pick-up through the cavity, after exciting it at the input. From this measurement, the resonance frequency can be easily obtained. To ensure accurate results, it is crucial to maintain a constant ambient pressure within the cryostat during this measurement, thereby preventing any frequency changes due to mechanical deformations. The cavities are initially parked at a specific starting temperature and pressure. A slow, non-adiabatic warm-up process is then initiated. Temperature data for this measurement is acquired from a Cernox® sensor attached to the outer surface of the cavity at the equator. Additionally, the temperature at the top and bottom of the cavity, along with the helium pressure, is continuously monitored and recorded during the warm-up process to assess the experimental procedure and ensure data quality. After RF tests, liquid helium is removed and df vs. T are measured during the warm-up process, in temperature range between 4.5 K and 12 K at a controlled rate of 0.5-1.5 K/h, while maintaining a stable pressure of 1111 mBar. During the measurement process, the resonance frequency in monitored using a Vector Network Analyzer (VNA). Adjusting the RF setup for the highest signal-to-noise ratio and a Lorentz distribution is fitted to obtain the resonance frequency. The entire spectrum at each temperature is recorded. Through the use of these techniques and data analysis methods, we can achieve precise and reliable df vs. T curve.

In our study, we have focused on investigating TESLA-shaped 1.3 GHz bulk niobium (Nb) single-cell SRF cavi-

* rezvan.ghanbari@desy.de

ISBN: 978-3-95450-234-9 ISSN: 2673-5504 doi:10.18429/JACoW-SRF2023-MOPMB021

ties [20]. In this paper, we present the results obtained from five cavities named 1DE19, 1AC2, 1DE18, 1RI4 and 1RI2. These cavities underwent baseline treatments [21, 22]. Then, cavity 1DE18 was coated with an 18 nm layer of Al_2O_3 using thermal atomic layer deposition (ALD) at 120 °C. This ALD coating served as an insulating layer, preventing the growth of the native oxide layer after subsequent heat treatment [23, 24]. Finally, all five cavities underwent mid-T heat treatment with different recipes (see Table 1). In addition, one conical sample with each cavity treated. Three of these samples, treated with 1DE19, 1AC2 and 1RI2, were analyzed using time-of-flight secondary ion mass spectrometry (TOF-SIMS) to determine the concentration of oxygen impurities present at a depth of up to 250 nm.

EFFECT OF MID-T HEAT TREATMENT ON df VS. T AND Q_0 VS. E_{ACC}

As expected, the local minimum after crossing T_c, the so-called dip, is observed in the df vs. T curves of our mid-T heat treated cavities. To have a comparable feature, we have plotted the frequency shift, f(T) versus reduced temperature scale, T/T_{c0}, relative to the normal conducting frequency, f_{NC}, serving as a reference and T_{c0} defines 9.27 K. Q_0 shows df vs. T/T_{c0} and Q_0 vs. E_{acc} for cavity 1DE18 before and after mid-T heat treatment. In Fig. 1 (a), the frequency behavior of the coated cavity shows no dip before the mid-T heat treatment, but a sharp transition from the superconducting to the normal conducting regime, as typical for cavities without mid-T heat treatment. After heating the cavity for 3 h at 300 °C, a dip with high magnitude, $\Delta f_{dip} = f_{NC} - f_{min}$, near T_c, and higher magnitude of total frequency shift, $\Delta f_0 = f(T=0) - f_{NC}$, are observed. These changes clearly demonstrate the impact of mid-T heat treatment on the behavior of df vs. T. Figure 1 (b) illustrates RF performance of 1DE18 in three steps, after the baseline treatment, after the coating of 18 nm Al_2O_3 and after the mid-T heat treatment. The Q_0 vs. E_{acc} curves show the typical behavior of a European XFEL cavity, even after coating, and that after mid-T heat treatment. To further analyze the dip features, we define ΔT_c as a temperature difference of points A and B in Fig. 1 (a), which is $\Delta T_c = T_{c,max} - T_{c,min}$. Point A and B are given by the intersection of f_{NC} extrapolated to lower T and the measured frequency response of the cavity. The intersection at the lower temperature gives the $T_{c,min}$, while the intersection at the higher temperature is the $T_{c,max}$. Definitions of dip features in this section is used in the subsequent section, enabling us to establish meaningful correlations between the dip and performance characteristics.

Δf_0, Δf_{dip} AND $Q_{0,max}$ CORRELATIONS

In this section, we explore the significance of oxygen concentration in relation to the frequency dip observed near T_c in mid-T heat-treated SRF cavities. We investigate how the evolution of frequency features is influenced by skilful adjustments in the duration and temperature of mid-T heat treatment, allowing us to understand better the impact of

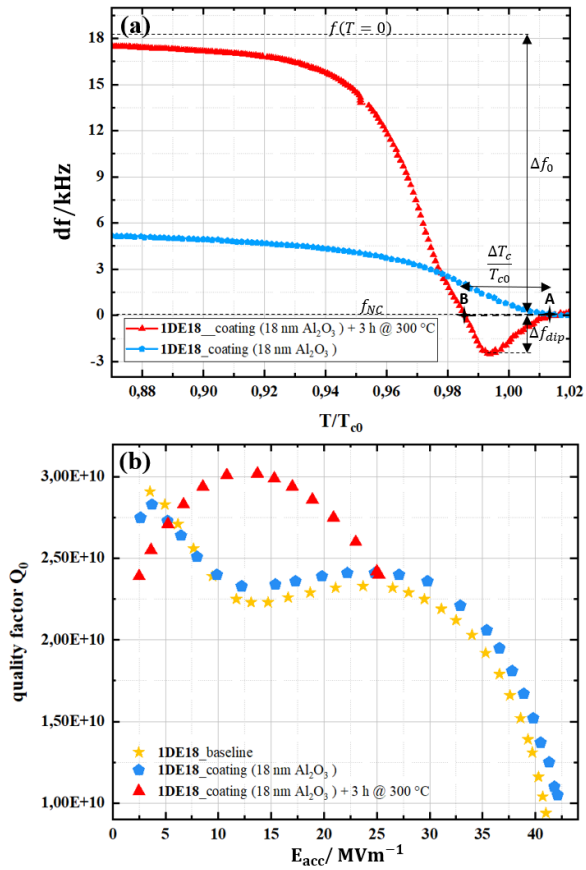

Figure 1: (a) Frequency shift versus reduced temperature scale and (b) Q_0 versus E_{acc} of 1DE18. The relative uncertainty for the measurement of the quality factor is below 10%. Points A and B define as ($T_{c,max}/T_{c0}$, f_{NC}=0) and ($T_{c,min}/T_{c0}$, f_{NC}=0), respective

heat factors on the oxygen profile. This, in turn, leads to an overall improvement in the quality factor. We have utilized five mid-T heat treated cavities, each prepared using different recipes, which are thoroughly summarized in Table 1. Figure 2 illustrates the frequency shift of these cavities. Part (a) of the figure presents the entire range of frequency shifts, while part (b) magnifies the region near T_c to highlight the dip features the RF corresponding to different recipes. The extrapolated frequency shift in Fig. 2 (a) is plotted relative to the penetration depth at 0 K, achieved by fitting df vs. T below the dip distribution down to low temperatures. With using the dependency of the frequency shift on the penetration depth which can be explained by Slater's theorem [25] and the penetration depth itself is dependent on temperature by Gorter-Casimir model [26], tending towards a constant value at lower temperatures. From our observation, we categorize the total frequency shifts, denoted as Δf_0, into three ranges. The first range, with Δf_0 approximately ranging in 11-12 kHz, comprises cavities 1DE19 and 1AC2 treated at approximately 300 °C for around 3 h. The second group, with Δf_0 ranging from 17-18 kHz, consists of the coated cavity 1DE18 treated at 300 °C for 3 h and the cavity 1RI4 with the same duration but at a lower temperature of 250 °C. Finally, 1RI3 with Δf_0 around 23 kHz.

ISBN: 978-3-95450-234-9 ISSN: 2673-5504 doi:10.18429/JACoW-SRF2023-MOPMB021

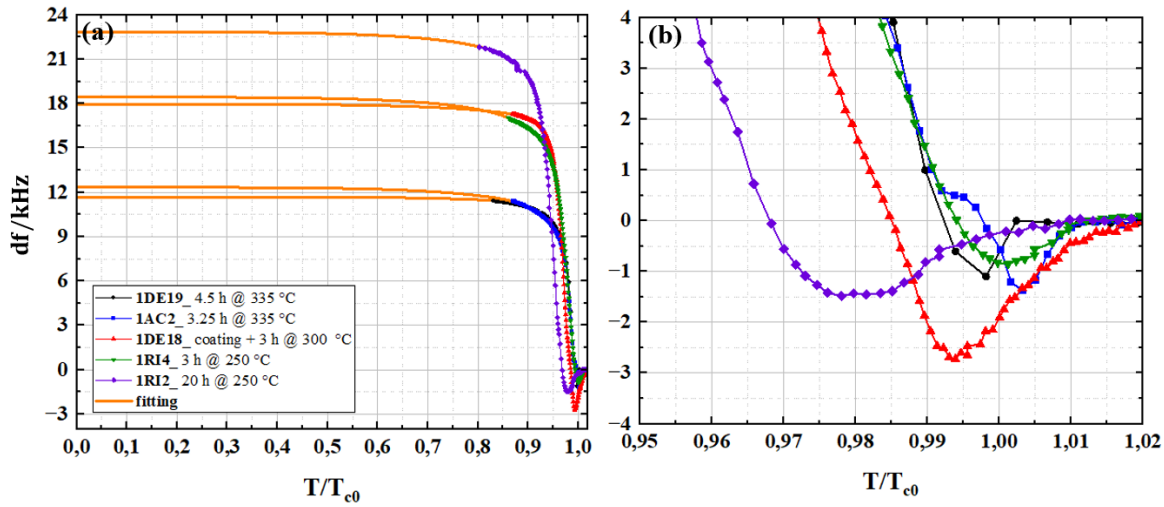

Figure 2: (a) Frequency shift versus T/T_{c0} in the range of superconducting area (b) magnified frequency shift versus T/T_{c0} near T/T_{c0}=1 for mid-T heat treated cavities.

The coated cavity shows the highest dip magnitude, as seen in Fig. 2 (b). We have observed similar dip behavior for cavities 1DE19 and 1AC2, which underwent similar recipes. Cavity 1RI4, treated at 250 °C with the same duration for 3 h, displays the lowest Δf_{dip} and exhibits a wide distribution near T_c. The final case, cavity 1RI2, subjected to the longest duration of heat treatment for 20 h at 250 °C, demonstrates the widest distribution of the dip near T_c, with ΔT_c measuring 0.38 K. To gain a better understanding of the various mid-T heat treated cavities, Fig. 3 demonstrates that cavity 1DE19 achieves the highest Q_0, followed by decreasing Q_0 values for cavities 1AC2, 1DE18, 1RI4, and 1RI2, respectively. Overall, we may conclude that the recipes involving higher temperatures and shorter durations yield superior performance in this study. To establish more elaborate correlations, we extract key parameter of the curves in Fig. 2 and Fig. 3, which are summarized in Table 1.

In Fig. 4, we present a comparison of the measured maximum Q_0 values with two important features of df vs. T.

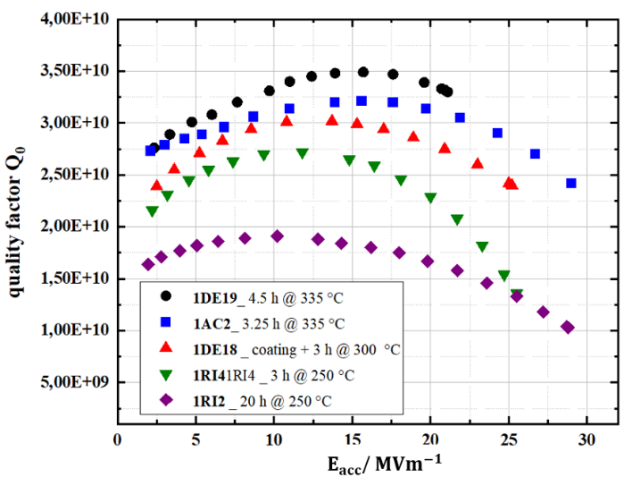

Figure 3: Q_0 versus E_{acc} of mid-T heat treated cavities, 1DE19, 1AC2, 1DE18, 1RI4, 1RI2 with different recipes.

In part (a), we have plotted Q_0 versus Δf_0 and in part (b),

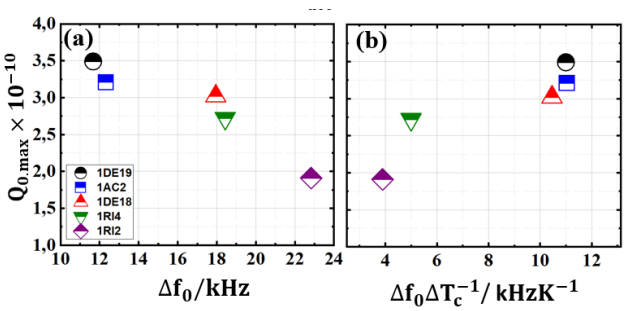

Figure 4: (a) the maximum of Q_0 at 2 K plotted versus total frequency shift, Δf_0 and (b) versus $\Delta f_{dip}/\Delta T_c$ (details in Table 1).

Q_0 versus $\Delta f_{dip}/\Delta T_c$ is plotted. It is evident that there is a clear relationship between $Q_{0,max}$ and Δf_0 with a decrease in the quality factor as the frequency shift increases. This correlation agrees well with previous studies on the effect of impurities to reduce mean free path and consequently increase the penetration depth of balk niobium [15]. Notably, we have observed a result where higher values of $\Delta f_{dip}/\Delta T_c$ correspond to cavities with higher $Q_{0,max}$. Actually, $\Delta f_{dip}/\Delta T_c$ shows the sharpness of dip distribution and it means higher sharpness correlates with the higher quality factor of cavities. Furthermore, we can discern a distinct separation between two groups of cavities that are around a specific magnitude of $\Delta f_{dip}/\Delta T_c$, with each group corresponding to a heat treatment recipe at the same temperature. The first group, including 1DE19, 1AC2, and 1DE18, was heated at around 300 °C, while the second group, comprising 1RI2 and 1RI4, underwent a heat treatment at approximately at 250 °C. This suggests a potential correlation between $\Delta f_{dip}/\Delta T_c$ of the dip distribution and heat treatment recipes with the same temperature. Although further statistical analysis is required to confirm this observation. If we assume that Nb surface after mid-T heat treatment is considered as composed of "compounds" of niobium and dissolved

ISBN: 978-3-95450-234-9 ISSN: 2673-5504 doi:10.18429/JACoW-SRF2023-MOPMB021

Table 1: Summary of df Versus T/T_{c0} and Q_0 Versus E_{acc} Features

Cavity	Heat treatment	$Q_{0,max}$ [$\times 10^{-10}$]	E_{acc} of $Q_{0,max}$ [MVm^{-1}]	Δf_0 [kHz]	Δf_{dip} [kHz]	ΔT_c [K]	$\Delta f_{dip}\Delta T_c^{-1}$ [kHz K^{-1}]
1DE19	4.5 h @ 335 °C	3.49	15.7	11.67	1.10	0.10	11.00
1AC2	3.25 h @ 335 °C	3.21	15.6	12.32	1.37	0.11	11.03
1DE18	coating + 3 h @ 300 °C	3.02	13.7	17.95	2.72	0.26	10.46
1RI4	3 h @ 250 °C	2.72	11.8	18.43	0.85	0.17	5.00
1RI2	20 h @ 250 °C	1.91	10.2	22.83	1.48	0.38	3.89

oxygen being embedded in niobium [27], dip behavior is caused by distribution of oxygen compounds which are created in bulk Nb structure during heat treatment [15–17, 27], the sharpness of the dip distribution might correlate with the size of the compounds and the depth till which those compounds are forming, where both are governed by the oxygen diffusion profile. With this assumption we can say that the temperature of heat treatment may determine the size of compounds or a depth distribution. Moreover, the dip magnitude might correlate with the concentration of these oxygen compounds. It is worth to mention that cavity 1DE18 which shows the highest amount of Δf_{dip} has the lowest BCS resistance of only 3 nΩ at 2 K and this intriguing observation compels us to hypothesize that the depth of the dip might correlate with the BCS resistance, highlighting the need for further in-depth investigations to figure out the captivating phenomenon behind it.

To delve deeper into this remarkable correlation, it is important to consider that both Q_0 and the dip features are intrinsically linked to the near surface oxygen concentration. Furthermore, as near T_c the penetration depth increases, the cavity behavior is more sensitive to a deeper part of the oxygen profile. Figure 5 shows NbO^+ concentration for the first 240 nm of three samples. Each of these samples was

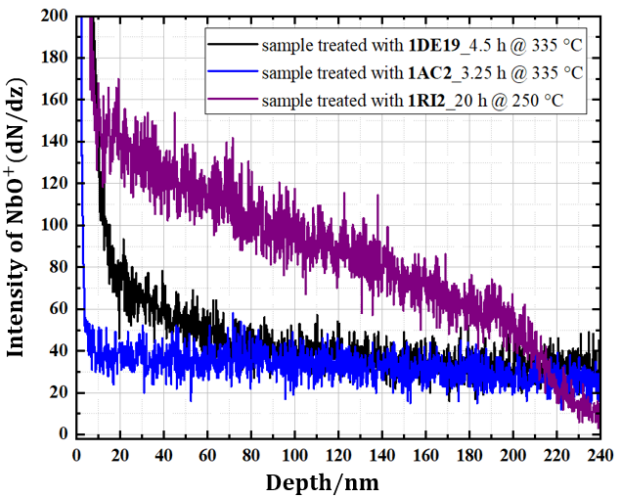

Figure 5: TOF-SIMS acquired depth profile of NbO^+.

treated together with a cavity, namely 1DE19, 1AC2 and 1RI2. 1DE19 and 1AC2, which show a similar behavior in terms of maximal Q_0 and for the dip features, also have a similar oxygen distribution except the first 60 nm, especially compared to 1RI2. Those oxygen distribution can be easily explained by the diffusion process and the different temperatures and times applied. The heat treatment for 3 h at 300 °C shows lower and no pronounce decreasing oxygen concentration compare to heat treatment for 20 h at 250 °C. It is evident that for the cavity with the largest frequency shift, 1RI2, which then translates into the largest effective penetration depth and therefore the smallest mean free path, the highest amount of interstitial oxygen is observed. The interesting result obtained from these analyses have been motivated us to extend our investigation to other samples treated with varying durations and temperatures with SIMS measurement. To gain further insights into these fascinating correlations, more statistics for df vs. T measurement are required. This will enable us to establish reliable correlations between the dip of the frequency shift, RF performance, and the near surface oxygen profile of the SRF cavities after mid-T heat treatment.

CONCLUSION

Systematic frequency vs. temperature measurements significantly contributes to our attempt to unveil underlying physics of heat treatments. Our investigation of correlations of the quality factor with the dip phenomena and the role of oxygen concentration near the surface in mid-T heat-treated cavities produced first promising results. Observed correlations, such as that the quality factor improves most when the frequency shift is smallest, indicate that the interstitial content is the cause for the improved RF behavior. By adjusting the duration and temperature of the applied heat treatments, therefore steering the near-surface oxygen concentration, the appearance and properties of the dip can be tuned. Furthermore, different maximal quality factors are observed for those different thermal budgets, fitting the assumption that the interstitial oxygen profile affects the surface resistance. In agreement to that, we observed that samples with a lower oxygen concentration were annealed with the better performing cavities. Moreover, our findings on coated cavity with the highest dip magnitude and R_{BCS} of 3 nΩ at 2 K, suggest a potential of correlation between the magnitude of dip and the BCS resistance, indicating the need for further investigations.

ACKNOWLEDGEMENT

The authors would like to thank T. Krokotsch, A. Sulimov, M. Wiencek, R. Zierold and the cleanroom and AMTF teams

ISBN: 978-3-95450-234-9 ISSN: 2673-5504 doi:10.18429/JACoW-SRF2023-MOPMB021

at DESY for preparing the cavities and performing the vertical tests. Also, we would like to thank S. Nouri Shirazi and T. Fladung for the SIMS measurement. This work is partially funded by Helmholtz Association within the topic Accelerator Research and Development (ARD) of the Matter and Technologies (MT) Program and from the BMBF project 05H21GURB2.

REFERENCES

[1] D. Bafia *et al.*, "Investigating the Anomalous Frequency Variations Near Tc of Nb SRF Cavities", in *Proc. SRF'21*, East Lansing, MI, USA, Jun.-Jul. 2021, pp. 885–892. doi:10.18429/JACoW-SRF2021-FROFDV03

[2] H. Hu, D. Bafia, and Y.-K Kim, "Examining the Effects of Oxygen Doping on SRF Cavity Performance", in *Proc. NA-PAC'22*, Albuquerque, NM, USA, Aug. 2022, pp. 196–198. doi:10.18429/JACoW-NAPAC2022-MOPA67

[3] Y. Zhitao *et al.*, "Effective medium temperature baking of 1.3 GHz single cell SRF cavities", *Physica C*, vol. 599, p. 1354092, Aug. 2022. doi:10.1016/j.physc.2022.1354092

[4] C. Bate *et al.*, "Recent mid-T single-cell treatments R&D at DESY", presented at SRF'23, Grand Rapids, MI, USA, Jun. 2023, paper MOPMB022, this conference.

[5] L. Steder *et al.*, "Medium Temperature Treatments of Superconducting Radio Frequency Cavities at DESY", in *Proc. LINAC'22*, Liverpool, UK, Aug.-Sep. 2022, pp. 840-843. doi:10.18429/JACoW-LINAC2022-THPOGE22

[6] G. Ciovati, "Effect of low-temperature baking on the radio-frequency properties of niobium superconducting cavities for particle accelerators", *J. Appl. Phys.*, vol. 96, no. 3, pp. 1591–1600, Aug. 2004. doi:10.1063/1.1767295

[7] S. Posen *et al.*, "Ultralow Surface Resistance via Vacuum Heat Treatment of Superconducting Radio-Frequency Cavities", *Phys. Rev. Appl.*, vol. 13, p. 014024, Jan. 2020. doi:10.1103/physrevapplied.13.014024

[8] F. He *et al.*, "Medium-temperature furnace baking of 1.3 GHz 9-cell superconducting cavities at IHEP", *Supercond. Sci. Tech.*, vol. 34, no. 9, p. 095005, Aug. 2021. doi:10.1088/1361-6668/ac1657

[9] Q. Zhou, F. S. He, W. Pan, P. Sha, Z. Mi, and B. Liu, "Medium-temperature baking of 1.3 GHz superconducting radio frequency single-cell cavity", *Radiat. Detect. Technol. Methods*, vol. 4, no. 4, pp. 507–512, Oct. 2020. doi:10.1007/s41605-020-00208-7

[10] H. Ito, A. Araki, and K. Umemori, "Systematic Investigation of Mid-T Furnace Baking for High-Q Performance", in *Proc. SRF'21*, East Lansing, MI, USA, Jun.-Jul. 2021, pp. 881–884. doi:10.18429/JACoW-SRF2021-FROFDV01

[11] F. Herman and R. Hlubina, "Microwave response of superconductors that obey local electrodynamics", *Phys. Rev. B.*, vol. 104, p. 094519, Sep. 2021. doi:10.1103/PhysRevB.104.094519

[12] E. M. Lechner *et al.*, "RF surface resistance tuning of superconducting niobium via thermal diffusion of native oxide", *Appl. Phys. Lett.*, vol. 119, no. 8, p. 082601, Aug. 2021. doi:10.1063/5.0059464

[13] M. Wenskat *et al.*, "Vacancy-Hydrogen Interaction in Niobium during Low-Temperature Baking", *Sci. Rep.*, vol. 10, p. 8300, May 2020, doi:10.1038/s41598-020-65083-0

[14] M. Wenskat *et al.*, "Vacancy dynamics in niobium and its native oxides and their potential implications for quantum computing and superconducting accelerators", *Phys. Rev. B*, vol. 106, p. 094516, Sep. 2022. doi:10.1103/physrevb.106.094516

[15] H. Ueki, M. Zarea, and J. A. Sauls, "The Frequency Shift and Q of Disordered Superconducting RF Cavities", *arXiv*, Jul 2022. doi:10.48550/arXiv.2207.14236

[16] M. Martinello *et al.*, "Effect of interstitial impurities on the field dependent microwave surface resistance of niobium," *Appl. Phys. Lett.*, vol. 109, no. 6, p. 062601, Aug. 2016. doi:10.1063/1.4960801

[17] G. D. L. Simone *et al.*, "Temperature dependent near-surface interstitial segregation in niobium", *J. Phys.: Condens. Matter*, vol. 33, p. 265001, 2021. doi:10.1088/1361-648X/abf9b7

[18] A. Grassellino *et al.*, "Nitrogen and argon doping of niobium for superconducting radio frequency cavities: a pathway to highly efficient accelerating structures", *Supercond. Sci. Tech.*, vol. 26, p. 102001, 2013. doi:10.1088/0953-2048/26/10/102001

[19] W. DeSorbo, "Effect of dissolved gases on some superconducting properties of niobium", *Phys. Rev.*, vol. 132, p. 107, 1963. doi:10.1103/PhysRev.132.107

[20] B. Aune *et al.*, "Superconducting TESLA cavities", *Phys. Rev. Spec. Top. Accel. Beams*, vol. 3, p. 092001, Sep. 2000. doi:10.1103/physrevstab.3.092001

[21] D. Reschke *et al.*, "Performance in the vertical test of the 832 nine-cell 1.3 GHz cavities for the European X-ray Free Electron Laser", *Phys. Rev. Accel. Beams*, vol. 20, p. 042004, Apr. 2017. doi:10.1103/PhysRevAccelBeams.20.042004

[22] L. Steder and D. Reschke, "Statistical Analysis of the 120 °C Bake Procedure of Superconducting Radio Frequency Cavities", in *Proc. SRF'19*, Dresden, Germany, Jun.-Jul. 2019, pp. 444-447. doi:10.18429/JACoW-SRF2019-TUP020

[23] M. Wenskat *et al.*, "Vacancy Dynamics in Niobium and Its Native Oxides and Their Potential Implications for Quantum Computing and Superconducting Accelerators", presented at SRF'23, Grand Rapids, MI, USA, Jun. 2023, paper TUIBA02, this conference.

[24] G. K. Deyu *et al.*, "Successful Al_2O_3 coating of superconducting niobium cavities by thermal ALD", presented at SRF'23, Grand Rapids, MI, USA, Jun. 2023, paper MOPMB016, this conference.

[25] L. C. Maier, Jr and J. C. Slater, "Field Strength Measurements in Resonant Cavities", *J. Appl. Phys.*, vol. 23, pp. 68–77, 1952. doi:10.1063/1.1701980

[26] C. Gorter and H. Casimir, "On supraconductivity I", *Physica*, vol. 1, pp. 306-320, 1934. doi:10.1016/S0031-8914(34)90037-9

[27] W. Weingarten, "Field-Dependent Surface Resistance for Superconducting Niobium Accelerating Cavities–Condensed Overview of Weak Superconducting Defect Model", *IEEE Trans. Appl. Supercond.*, vol. 33, p. 3500309, 2023. doi:10.1109/TASC.2023.3243268